Heteroatom Chemistry
Volume 10, Number 6, 1999

Synthesis of Spiropyrrolidines: 1,3-Dipolar Cycloaddition Reactions of an Azomethine Ylide to Unusual Dipolarophiles; A Molecular Orbital Study of the Cycloaddition Reaction

A. Amal Raj,[1] R. Raghunathan,[1] and E. J. P. Malar[2]

[1]*Department of Organic Chemistry, University of Madras, A. C. College Campus, Chennai 600 025, Tamil Nadu, India*

[2]*Department of Physical Chemistry, University of Madras, A. C. College Campus, Chennai 600 025, Tamil Nadu, India*

Received 11 April 1999

ABSTRACT: *A simple and efficient method for the synthesis of novel spiropyrrolidines has been accomplished by regioselective 1,3-dipolar cycloaddition reactions of an azomethine ylide generated by thermal-ring opening of cis-1-cyclohexyl-2-phenyl-3-benzoyl aziridine with various (E)-3-arylidene-4-chromanones. The synthesis proceeds in good yield to afford novel spiropyrrolidines, 1-cyclohexyl-2-phenyl-3-aryl-5-benzoylpyrrolidine-spiro-[4.3']4'-chromanones. The X-ray crystal structure analysis of one of the products confirms its structure. Molecular orbital calculations were performed to investigate the regioselectivity of the cycloaddition process.* © 1999 John Wiley & Sons, Inc. Heteroatom Chem 10: 500–507, 1999

INTRODUCTION

Pyrrolidines are among the most common structures in biologically active natural products. The diversity of their biological function (as well as their structures) has stimulated efforts for the synthesis of this class of compounds [1]. Among the various synthetic strategies, 1,3-dipolar cycloaddition reactions of azomethine ylides occupy a unique position in the synthesis of pyrrolidines [2].

A number of methods have been developed for the generation of ylides such as the desilylation approach conceived by Vedejs [3] and the tautomerism route by Grigg [4]. The generation of azomethine ylides by thermolysis of aroyl aziridines has attracted considerable attention because of the potential of these compounds to give pyrrolidine derivatives by electrocyclic ring opening and their ability to cycloadd to olefinic compounds. The intermolecular cycloaddition of azomethine ylides generated by the aziridine route has been extensively studied by Huisgen [5], Padwa [6] and others [7], and generalities concerning the regiochemical and stereochemical outcome of these cycloadditions have been well established [8].

In this article, we present an efficient synthesis of spiropyrrolidines by the 1,3-dipolar cycloaddition reaction of an azomethine ylide with the unusual dipolarophiles, (*E*)-3-arylidene-4-chromanones. Molecular orbital calculations predicted the regioselectivity of the cycloaddition process. (*E*)-3-Arylidene-4-chromanones were used for the first

Correspondence to: R. Raghunathan. E-mail: *rrnathan@unimad.ernet.in.*
Contract Grant Sponsor: CSIR, New Delhi.
Contract Grant Sponsor: UGC, New Delhi.
 CCC 1042-7163/99/060500-08

time both as a dienophile and dipolarophile in the synthesis of various polycyclic heterocyclic systems [9,10].

Like other dipolarophiles, arylidene chromanones are electron deficient and poised for facile cycloaddition reactions to yield novel spiroadducts. It is found that these compounds are moderately active and give highly selective products in all the cycloadditions that we have studied [9,10].

RESULTS AND DISCUSSION

In the present study, refluxing a solution of *cis*-1-cyclohexyl-2-phenyl-3-benzoylaziridine **2** with various (*E*)-3-arylidene-4-chromanones (**1a–f**) resulted in the formation of novel spiropyrrolidines (**3a–f**) (Table 1) in good yield (Scheme 1).

The reaction occurs by conrotatory ring opening of the *cis* aziridine to generate the azomethine ylide, which adds to the exocyclic double bond of (*E*)-3-arylidene-4-chromanones to give the cycloadducts. The reactions give a single product as evidenced by thin-layer chromatography (TLC) and yield novel 1-cyclohexyl-2-phenyl-3-aryl-5-benzoylpyrrolidine-spiro[4.3′] 4′-chromanones (**3a–f**).

The regiochemistry of cycloaddition was established by NMR spectroscopy. Thus, the H NMR spectrum of product **3a** exhibited peaks at δ 0.66–1.39 (m, H, cyclohexyl), 2.44 (m, N-CH), 3.48 (d, J = 13Hz, H_c), 4.17 (d, J = 13Hz, H_b), 5.10 (s, H_a), 5.43 (d, 1H, 10Hz, OCH_2), 4.58 (d, 1H, J = 10Hz, OCH_2) and 6.43–8.20 (m, 19H, aromatic) (Table 2). The larger coupling constant (13 Hz) for the protons H_b and H_c indicates that they are *trans* [11]. The ^{13}C spectrum of the product accords with this expectation (Table 3). Finally, X-ray crystal structure analysis of the product confirms the assigned structure.

It is noteworthy that the cycloaddition produces single stereoisomers. This suggests that the ylide that was generated in the reaction adopts only one of the two possible conformations and that because the geometry of the dipolarophile is fixed, it is presumed that the *trans* conformation of the ylide reacts regioselectively to give the adduct.

The high stereoselectivity observed in the cycloadditions indicates that a unique ylide geometry and transition state orientation are involved in the cycloaddition process. Molecular orbital calculations are in agreement with the observed regioselectivity.

MOLECULAR ORBITAL ANALYSIS

The reactivity of the chromanone derivatives **1a–f** with the dipole **2** has been examined by quantum chemical investigations at the semiempirical level. The computations were performed using the AM1 [12] and PM3 [13] methods, incorporated in the Gaussian 94 (version D.3) [14]. The reactant molecules were subjected to complete structural optimization using the Berni algorithm. At the optimized geometries of the reactant molecules, the electronic properties of the interacting frontier molecular orbitals (HOMO and LUMO) were analyzed. It may be mentioned that similar analysis was performed earlier for the 1,3-dipolar cycloaddition of diphenylnitrilimine with (*E*)-3-arylidene-4-chromanones [9] (R = H, Me, NO_2) and (*E*)-3-arylidene butenolides [15].

The energies of the HOMO and LUMO and the corresponding MO coefficients at the reactive sites

TABLE 1 Spiropyrrolidines **3a–f**

Product	*Yield (%)*	*m.p. (°C)*	*IR (KBr) νC=O (cm^{-1})*	*MS (70 eV) m/z (M^+)*	*Molecular Formula*	*Analysis Calcd/Found*		
						C	*H*	*N*
3a	51	179–181	1673, 1686	541	$C_{37}H_{35}O_3N$	82.07	6.47	2.58
						82.12	6.45	2.55
3b	63	174–176	1673, 1689	555	$C_{38}H_{37}O_3N$	82.16	6.67	2.57
						82.12	6.63	2.48
3c	59	180–181	1673, 1686	571	$C_{38}H_{37}O_4N$	79.86	6.48	2.45
						78.86	6.43	2.48
3d	93	182–183	1673, 1689	575	$C_{37}H_{34}O_3NCl$	77.22	5.88	2.44
						77.24	5.86	2.40
3e	50	214–116	1673, 1686	584	$C_{39}H_{40}O_3N_2$	80.14	6.85	4.79
						80.12	6.88	4.46
3f	55	206–207	1673, 1689	586	$C_{37}H_{34}O_5N_2$	75.77	5.80	4.78
						75.76	5.78	4.80

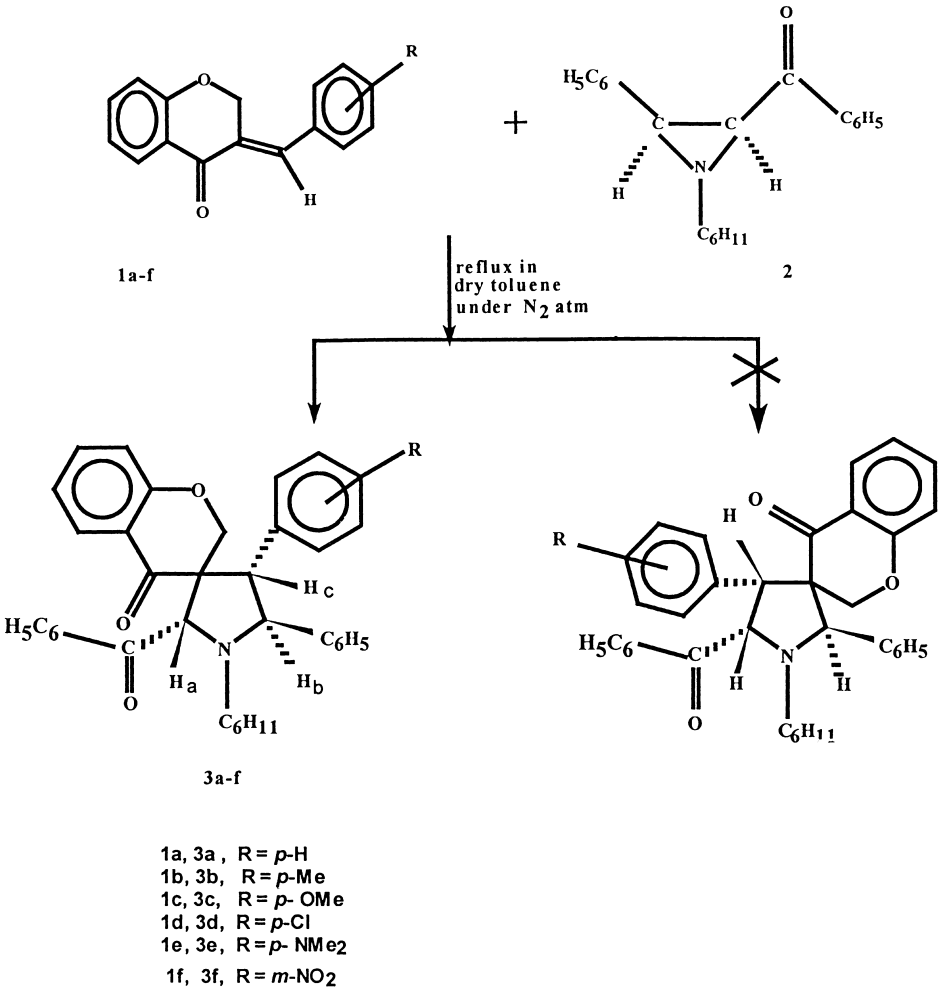

SCHEME 1

TABLE 2 ^{1}H NMR δ Values ($CDCl_3$/TMS) of **3a–3f**[a]

						Cyclohexyl Ring	
Product	*Aromatic Region*	*OCH_2*	*H_a*	*H_b*	*H_c*	*N-CH*	*$-CH_2$*
3a	6.43–8.20 (m, 19H)	5.43 (d 1H, 10Hz) 4.58 (d, 1H, 10Hz)	5.10(s)	4.17 (d, 13Hz)	3.48 (d, 13Hz)	2.48 (m, 1H)	0.66–1.39 (m, 10H)
3b	6.42–8.17 (m, 18H)	5.39 (d, 1H, 10Hz) 4.49 (d, 1H, 10Hz)	5.07(s)	4.16 (d, 13Hz)	3.49 (d, 13Hz)	2.50 (m, 1H)	0.66–1.23 (m, 10H)
3c	6.42–8.17 (m, 18H)	5.37 (d, 1H, 10Hz) 4.45 (d, 1H, 10Hz)	5.07(s)	4.16 (d, 13Hz)	3.50 (d, 13Hz)	2.46 (m, 1H)	0.66–1.37 (m, 10H)
3d	6.49–8.20 (m, 18H)	5.34 (d, 1H, 11Hz) 4.42 (d, 1H, 11Hz)	5.10(s)	4.13 (d, 12Hz)	3.50 (d, 12H)	2.50 (m, 1H)	0.64–1.44 (m, 10H)
3e	6.50–8.27 (m, 18H)	5.39 (d, 1H, 10Hz) 4.48 (d, 1H, 10Hz)	5.11(s)	4.21 (d, 2Hz)	3.51 (d, 12Hz)	2.54 (m, 1H)	0.73–1.29 (m, 10H)
3f	6.51–8.38 (m, 18H)	5.41 (d, 1H, 11Hz) 4.60 (d, 1H, 11Hz)	5.15(s)	4.10 (d, 13Hz)	3.50 (d, 13Hz)	2.48 (m, 1H)	0.66–1.39 (m, 10H)

[a]δ values for the substituents in **3b**: R = *p*-Me-2.27(s), **3c**: R = *p*-OMe-3.74(s), **3e**: R = *p*-NMe_2-2.94(s)

are shown in Tables 4 and 5, respectively, for the (*E*)-3-arylidene-4-chromanones. The HOMO of the *m*-nitro derivative is largely delocalized over the phenyl ring of the arylidene chromanone that results in a small contribution at the reactive C = C double bond site. However, the next lower MO (MO. No. 51) has a significant contribution at the reactive site, and the values are included in Table 4. It is seen that the energies of the HOMO and LUMO are raised by the presence of an electron-donating substituent, and the energy levels show a drastic decrease when the electron-withdrawing nitro group is present. The PM3 results do not show much change in the Frontier orbital energies for the *N,N*-dimethyl derivative. The MO coefficients do not vary significantly with the nature of the substituents except in the nitro derivative wherein both HOMO and LUMO coefficients are reduced.

The optimized bond lengths and bond angles at the reactive site of the dipole intermediate **2b** (Figure 1) are shown in Table 6. At the AM1-optimized geometry of **2b**, we also performed single-point SCF MO calculation with the STO-3G basis set and performed Natural Bond Orbital analysis [16–18]. The Wiberg bond orders at the reactive site **2b** are listed in Table 6. The optimized bond lengths and bond orders clearly indicate that covalent bonding between the carbon centres C_1 and C_3 is very small; the covalent bond order is 0.23. The C_1N_2 bond exhibits partial double bond character with a bond order of 1.51.

Because we wanted to quantify the polarity of the atoms at the reactive site, the net charges were calculated using natural population analysis (NPA) with the STO-3G basis. The natural charges are reported to be more reliable than those obtained by

TABLE 3 ^{13}C NMR values ($CDCl_3$/TMS) of **3a–3f**

Product	δ Values (ppm)
3a	25.66, 25.88, 26.18, 29.96, 32.24, 54.64, 55.63, 56.66, 63.00, 70.10, 71.40, 117.62, 119.71, 121.57, 127.05, 127.26, 128.02, 128.18, 128.44, 128.55, 130.22, 133.12, 133.55, 136.24, 137.64, 141.86, 160.67, 192.88, 205.14
3b	25.62, 25.85, 26.15, 29.95, 32.19, 54.02, 55.60, 56.52, 62.88, 70.44, 71.22, 117.63, 119.59, 121.69, 127.43, 128.05, 128.29, 128.40, 128.46, 128.61, 131.61, 132.89, 133.25, 134.92, 135.67, 137.52, 141.53, 160.59, 192.65, 205.16.
3c	21.32, 25.98, 26.21, 26.51, 30.28, 32.56, 54.60, 55.96, 55.93, 63.32, 70.37, 71.76, 117.94, 120.08, 121.84, 127.53, 128.34, 128.50, 128.76, 128.87, 129.23, 130.39, 133.41, 135.83, 136.87, 138.01, 142.30, 161.02, 193.32, 205.51
3d	25.70, 25.91, 26.20, 29.98, 32.25, 53.94, 54.03, 55.08, 55.69, 56.63, 63.04, 70.40, 71.49, 117.61, 119.78, 121.57, 127.23, 128.06, 128.20, 128.41, 128.58, 131.27, 133.13, 135.55, 137.69, 142.03, 160.71, 193.06, 205.28
3e	25.71, 25.94, 26.23, 30.01, 32.28, 40.49, 54.00, 55.69, 56.78, 63.10, 70.09, 71.58, 117.65, 119.87, 121.43, 123.77, 127.08, 128.03, 128.14, 128.41, 128.52, 130.86, 133.03, 135.42, 137.76, 142.33, 149.47, 160.77, 193.30, 205.28
3f	25.60, 25.82, 26.12, 30.01, 32.16, 54.25, 55.57, 56.55, 62.78, 70.64, 71.02, 117.60, 119.46, 121.92, 125.21, 127.73, 128.14, 128.31, 128.46, 128.55, 129.22, 133.41, 135.88, 136.43, 136.87, 137.37, 141.03, 148.19, 160.50, 192.24, 204.84

TABLE 4 Energy of the HOMO and the MO Coefficients at the Reactive Sites (**1a–f**)

				HOMO Coefficients			
		HOMO Energy (eV)		*C1*		*C2*	
R	*HOMO M.O. No*	*AM1*	*PM3*	*AM1*	*PM3*	*AM1*	*PM3*
H	44	−9.24	−9.35	0.20	0.21	0.15	0.16
Me	47	−9.17	−9.26	0.29	0.31	0.19	0.22
OMe	50	−9.01	−9.06	0.34	0.31	0.19	0.21
Cl	47	−9.37	−9.30	0.22	0.29	0.16	0.21
NMe_2	53	−8.57	−9.33	0.26	0.24	0.12	0.18
NO_2	52	−9.52	−9.61	0.08	0.10	0.10	0.08
	51	−10.16	−10.16	0.36	0.37	0.29	0.33

TABLE 5 Energy of the LUMO and the MO Coefficients at the Reactive Sites (**1a–f**)

				LUMO Coefficients			
		LUMO Energy (eV)		*C_1*		*C_2*	
R	*LUMO MO No.*	*AM1*	*PM3*	*AM1*	*PM3*	*AM1*	*PM3*
H	45	−0.76	−0.80	−0.37	−0.35	0.46	0.42
Me	48	−0.74	−0.78	−0.37	−0.36	0.46	0.42
OMe	51	−0.53	−0.76	−0.36	−0.34	0.46	0.42
Cl	48	−0.92	−0.93	−0.39	−0.36	0.49	0.41
NMe_2	54	−0.67	−0.83	−0.36	−0.36	0.46	0.42
NO_2	53	−1.37	−1.41	−0.26	−0.25	0.25	0.23

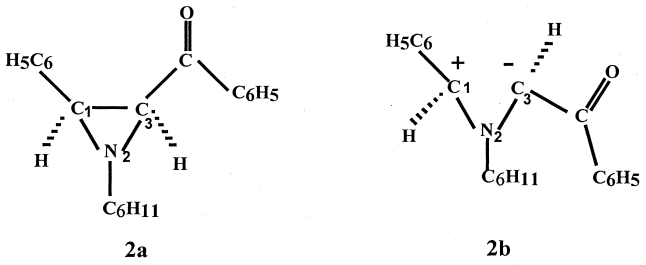

FIGURE 1 Reactive site of the dipole.

TABLE 6 Optimized Bond Lengths (bond orders) and Bond Angle at the Reactive Site **2b**

	Bond Length in A (Bond orders)[a]	
	AM1	*PM3*
C_1C_3	2.318 (0.23)	2.320
C_1N_2	1.336 (1.51)	1.336
N_2C_3	1.370 (1.18)	1.375
	Bond angle (°)	
	AM1	PM3
$C_1N_2C_3$	118.0	117.7

[a]Wiberg bond orders were obtained from NBO program using STO-3G calculation at AM1 geometry.

Mulliken population analysis (MPA). The NPA and MPA charges are +0.05 and +0.04 on carbon 1.

The carbon center 3 has the negative change of the dipole with the corresponding charges −0.17 and −0.11, respectively. Table 7 shows the HOMO and LUMO energies and their coefficients at the reactive site in **2b**. The orbital energies show that the interaction between the HOMO of the 1,3-dipole with the LUMO of the chromanone derivative is more favorable than that between the HOMO of the chromanone derivative with the LUMO of the 1,3-dipole because the energy gap between the latter and the former exceed 1.5 eV.

TABLE 7 Frontier Orbital Energies and Coefficients for the 1,3-dipole **2b**

	HOMO		*LUMO*	
	AM1	*PM3*	*AM1*	*PM3*
Energy	−7.68	−8.15	−0.46	−0.57
MO Coefficients				
C_1	0.52	0.49	+0.45	0.43
N_2	0.01	0.02	−0.48	−0.53
C_3	−0.35	−0.33	0.08	0.08

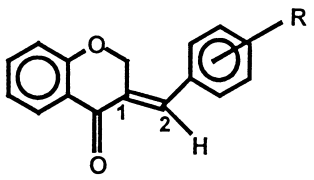

FIGURE 2 Reactive sites (**1a–f**).

Calculation of the atomic coefficients of the dipolarophile by both AM1 and PM3 methods reveal that HOMO coefficients of the olefinic carbons are comparable in magnitude. In all the cases (**1a–f**), it is seen that the LUMO coefficient of the olefinic carbon C_1 of the dipolarophile is comparable in value with that of the cationic carbon in the 1,3-dipole, and the coefficient of the C_2 carbon to that of the anionic carbon of the dipole results in an overlap between these corresponding orbitals leading to the formation of the observed regioisomer. Thus, the molecular orbital concept explains the regiochemistry of this cycloaddition.

The MO correlation diagram for the interaction between **1a** and **2b** is shown in Figure 3 using the AM1 energies. We have also optimized the geometry of the product formed in the cycloaddition of **1a** (R = H) with **2b**, the optimized AM1 geometrical pa-

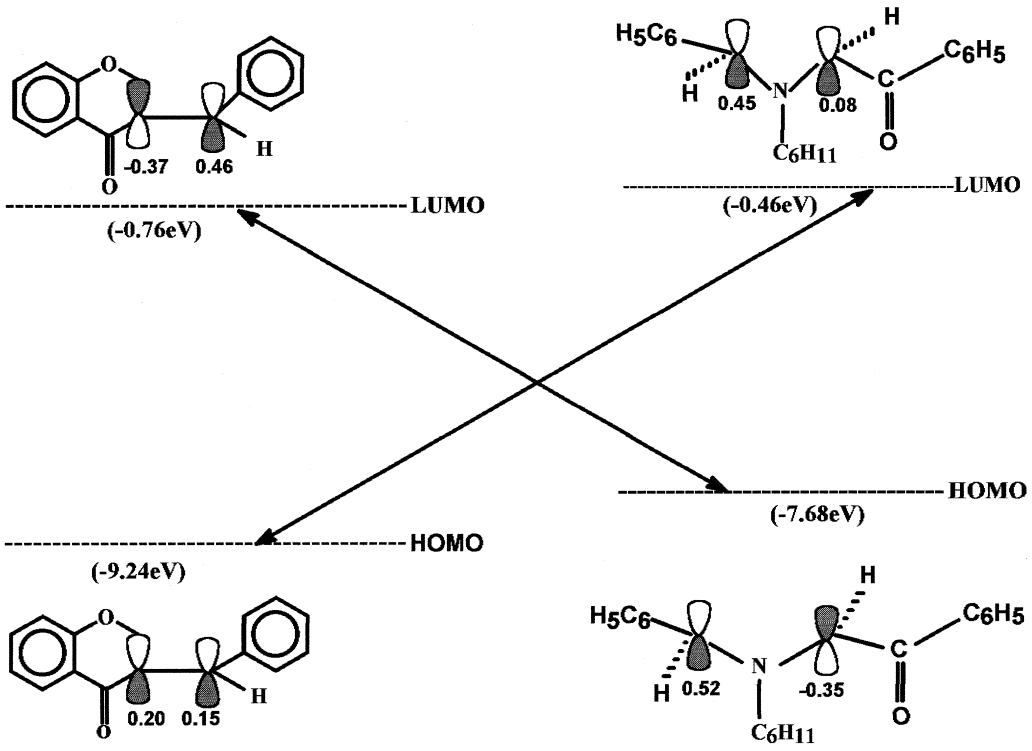

FIGURE 3 Correlation diagram.

rameters being compared with the crystallographic structure (Figure 4) in Table 6. There is good agreement between the calculated and experimental geometries. The AM1 calculation predicts the enthalpy of formation of **3a** to be 24.95 kcal/mol.

Crystal Data for Compound **3a**

Molecular Formula: $C_{37}H_{35}O_3N$. Molecular weight 541, monoclinic, space group = P_{21}/c, a = 14.021(0.0030), b = 18.682(0.0040), c = 11.362(0.0020), Dc = 1.3072 g/cm^3, V = 2961.69, α = 90° (0.00), β = 95.75° (0.00), γ = 90° (0.00). *Mo* Kα radiation, λ = 0.71073 Å, μ = 0.813 cm^{-1}, F(000) = 892. The crystal is yellow and square-shaped. Number of atoms = 76.

A crystal with dimensions of 0.31 × 0.25 × 0.20 mm was used for X-ray data collection at 293 K on an ENRAF-NONIUS CAD4 diffractometer using molybdenum radiation and a graphite monochromator. A total of 5383 independent reflections for $2\theta_{max}$ = 50.6° were measured, out of which 3794 were considered. The structure was solved by direct methods using the program SHELXS86 [19].

The structure was refined by the full matrix least-squares method using SHELXL93 [20]. The final R indices are R = 0.0658 (6.58%). All the nonhydrogen atoms were refined anisotropically. All the hydrogens were located from the difference Fourier map. The maximum shift/e.s.d was 0.002 min, and maximum values in the final difference electron density maps are 0.37 and 0.55 e/Å^3. Atomic scattering factors were taken from international tables [21].

EXPERIMENTAL

All the melting points are uncorrected. The IR spectra were recorded on an IR-470 Shimadzu instrument. ^{1}H and ^{13}C NMR spectra were recorded in $CDCl_3$ using TMS as an internal standard on JOEL FX 90 Q at 90 MHz and JOEL GX 400 at 100.4 MHz instruments, respectively. Elemental analyses were performed on a CEST 1106 instrument. Mass spectra were recorded on a JOEL DX 303 HF spectrometer with a MASPEC system (MSW/9629)

All the (*E*)-3-arylidene-4-chromanones [9] and aziridine [22] reported here were prepared as per the literature procedures.

General Procedure

Reaction of (*E*)-3-arylidene-4-chromanones with *cis*-1-cyclohexyl-2-phenyl-3-benzoyl aziridine: a mixture

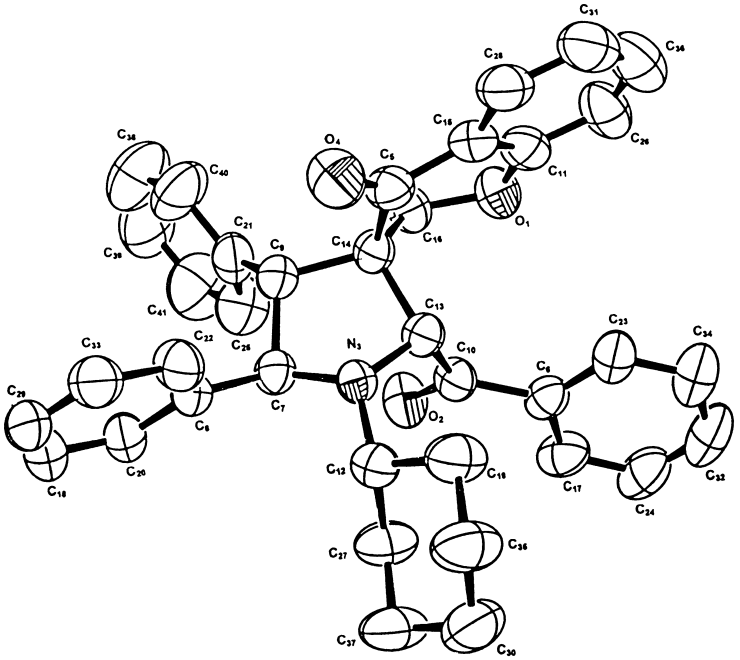

FIGURE 4 ORTEP diagram of **3a**.

of (*E*)-3-arylidene-4-chromanone and aziridine was refluxed in toluene under a nitrogen atmosphere for 48 hours. After the reaction was complete the solvent was evaporated in vacuo, and the resulting crude product was purified by column chromatography using a hexane–benzene mixture (70:30) as eluent. The product crystallized from ethanol as yellow needles. The spectral details for **3a–f** are reported in Tables 2 and 3. The selected bond angles and lengths for **3a** are shown in Table 8.

TABLE 8 Selected Bond Lengths and Bond Angles for Compound **3a** (Excluding H Atoms)

	Bond angle (°)			*Bond length (A)*	
Type	*Observed*	*Theoretical (AM1)*	*Type*	*Observed*	*Theoretical (AM1)*
C_{11}-O_1-C_{16}	115.88 (0.19)	114.3	O_1-C_{11}	1.3515	1.380
O_4-C_5-C_{14}	123.80 (0.11)	122.7	O_1-C_{16}	1.4443	1.434
O_4-C_5-C_{15}	121.34 (0.28)	122.5	O_4-C_5	1.2104	1.236
O_1-C_{11}-C_{26}	117.48 (0.20)	116.4	N_3-C_7	1.4675	1.478
O_1-C_{11}-C_{15}	122.01 (0.11)	122.5	N_3-C_{12}	1.4589	1.458
N_3-C_{12}-C_{27}	111.21 (0.20)	112.8	N_3-C_{13}	1.4489	1.468

ACKNOWLEDGMENTS

A. R. thanks University of Madras for the award of URF. We acknowledge RSIC, IIT, Madras for some of the spectral data reported here. We are thankful to Prof. D. Velmurugan and S. Thinagar from the Department of Crystallography and Biophysics at the University of Madras for X-ray analysis.

REFERENCES

[1] (a) Pearson, W. H. Ed. Advances in Heterocyclic Natural Product Synthesis, JAI Press Inc: Greenwich, 1990; Vol. 1; (b) Pichon, M. Tetrahedron Asymmetry 1996, 7, 927; (c) Ishibasi, H.; Sato, T.; Ikeda, M. J Synth Org Chem Jpn 1995, 53, 85; (d) Hudlicky, T.; Seoane, G.; Price, J. D.; Gadamasetti, K. G. Syn Lett 1990, 433.

[2] (a) Lown, J. W. 1,3-Dipolar Cycloaddition Chemistry; Padwa A, Ed.; John Wiley & Sons: New York, 1984; Vol. 1, pp 653; (b) Vedejs, E. Advances in Cycloaddition; Curran, D. P. Ed.; JAI Press Inc.: Greenwich, 1990; Vol. 1, pp 33; (c) Padwa, A.; Schoffstall, A. M. Advances in Cycloaddition; Curran, D. P. Ed; JAI Press Inc.: Greenwich, 1990; Vol. 2, pp 1.

[3] Vedejs, E.; West, F. G. Chem Rev 1986, 86, 941.

[4] Grigg, R.; Kemp, J. J Chem Soc Chem Comm 1988, 53, 1384.

[5] Huisgen, R.; Scheer, W.; Mader, H. Angew Chem Int Ed Engl 1969, 8, 602.

[6] Padwa, A.; Clough, S.; Glazer, E. J Am Chem Soc 1970, 92, 1778.

[7] (a) Grigg, R.; Kemp, J.; Sheldrick, G.; Trotter, J. J Chem Soc Chem Comm 1978, 108; (b) Lown, J.; Matsumato, K. J Org Chem 1971, 36, 1405; (c) Heine, H. W.; Henzel, R. P. J Org Chem 1969, 36, 1969.

[8] (a) Confalone, P. N.; Huje, E. M.; J Org Chem 1983, 48, 2994; (b) Padwa, A.; Hoffmann, G.; Tomas, M. Tetrahedron Lett 1983, 4303.

[9] Raghunathan, R.; Shanmugasundram, M.; Bhanumathi, S.; Malan, E. J. P. Heteroatom Chem 1998, 9, 327.
[10] Raghunathan, R.; Shanmugasundram, M., unpublished observations.
[11] Deshong, P.; Kell, D. A.; Sidler, D. R. J Org Chem 1985, 20, 2309.
[12] Dewar, M. J. S.; Zoebisch, E. G.; Healy, E. F.; Stewart, J. J. P. J Am Chem Soc 1985, 107, 3902.
[13] Stewart, J. J. P. J Comp Chem 1989, 10, 209–221.
[14] Frish, M. J.; Trucks, G. W.; Schlegel, H. B.; Gill, P. M. W.; Johnson, B. G.; Robb, M. A.; Cheeseman, J. R.; Keith, T.; Peterson, A.; Montgomery, J. A.; Raghavachari, K.; Al-Laham, M. A.; Zakrzewski, V. G.; Ortiz, J. V.; Foreseman, J. B.; Closlowski, I.; Stefanov, B. B.; Nanayakkara, A.; Challacombe, M.; Peng, C. Y.; Ayala, P. Y.; Chen, W.; Andres, J. L.; Replogle, E. S.; Gomperts, R.; Martin, R. L.; Fox, D. J.; Binkley, S.; Defrees, D. J.; Baker, J.; Stewart, J. P.; Gordon, N. H.; Gonzalez, C.; Pople, J. A. Gaussian, Inc., Pittsburgh, PA, 1995.
[15] Shanmugasundaram, M.; Raghunathan, R.; Malar, E. J. P. Heteroatom Chem 1998, 9, 517.
[16] Glendening, E. D.; Reed, A. E.; Carpenter, J. E.; Weinhold, F. NBO version 3.1.
[17] Foster, J. P. P., Weinhold, F. J Am Chem Soc 1980, 102, 7211.
[18] Reed, A. E.; Curtiss, L. A.; Weinhold, F. Chem Rev 1988, 88, pp 899–926.
[19] Sheldrick, G. M. SHELXS86, Programme for the solution of crystal structures; University of Gottingen, Germany (1993).
[20] Sheldrick, G. M.; SHELXL93, Programme for the refinement of crystal structures; University of Gottingen, Germany, 1993.
[21] International Tables for X-ray crystallography, Vol. C, 1992.
[22] Cromwell, N. H.; Babson, R. D.; Harris, C. E. J Am Chem Soc 1943, 65, 312.